EUROPEAN LABORATORY FOR PARTICLES PHYSICS (CERN)

Abstract ID-177
ALEPH 2003-015
CONF 2003-011
July 10, 2003

PRELIMINARY

Measurement of Triple Gauge-Boson Couplings in e^+e^- collisions from 183 to 209 GeV

The ALEPH Collaboration

Contact persons:
T. Barklow (timb@slac.stanford.edu)
S. Jezequel (jezequel@lapp.in2p3.fr)

Abstract

Triple gauge-boson couplings involving W-pairs are determined using data samples collected with the ALEPH detector at centre-of-mass energies between 183 and 209 GeV, corresponding to integrated luminosities of 684 pb^{-1}. The couplings, g_1^Z, κ_γ and λ_γ, are measured using an optimal observable method for W-pair events. Each coupling is measured individually while the two others are fixed at their Standard Model value. Including single-W and single-γ production, 95% confidence level intervals are:

$$\begin{aligned} 0.965 < \; g_1^Z \; < \; 1.099 \\ 0.861 < \; \kappa_\gamma \; < \; 1.140 \\ -0.048 < \; \lambda_\gamma \; < \; 0.081. \end{aligned}$$

Results are also presented for the cases where two or all three couplings are allowed to vary. An additional analysis using W-pair events is performed to set limits on the real and imaginary parts of all 14 triple gauge-boson couplings and to perform an indirect search for a techni-ρ resonance. No deviations from the Standard Model expectations are observed and the lower limit on the techni-ρ mass is 625 GeV at 95% C.L.

(*ALEPH contribution to 2003 LP03 and EPS HEP 2003*)

1 Introduction

The existence of the triple gauge-boson couplings (TGC) is a direct consequence of the $\mathrm{SU(2)_L \times U(1)_Y}$ structure of gauge theory. The measurement of the TGCs represents a fundamental test of the non-Abelian nature of the Standard Model. The triple $\gamma\mathrm{W^+W^-}$ and $\mathrm{ZW^+W^-}$ couplings have been studied with ALEPH in e^+e^- collisions at energies above the W-pair production threshold, using direct W-pair production ($e^+e^- \to \mathrm{W^+W^-}$) [1, 2], single-W production ($e^+e^- \to \mathrm{W}e\nu$) [3] and single-$\gamma$ production ($e^+e^- \to \nu\overline{\nu}\gamma(\gamma)$) [1]. In this paper, updated results on TGCs from analyses of W-pair final states using data recorded by the ALEPH detector between 183 and 209 GeV are presented.

The most general Lorentz invariant parametrisation of the $\gamma\mathrm{W^+W^-}$ and $\mathrm{ZW^+W^-}$ vertices can be described by 14 independent complex couplings [4–6], 7 for each vertex: $\mathrm{g_1^V}$, $\mathrm{g_4^V}$, $\mathrm{g_5^V}$, κ_V, λ_V, $\tilde{\kappa}_\mathrm{V}$ and $\tilde{\lambda}_\mathrm{V}$, where V denotes either γ or Z. Assuming electromagnetic gauge invariance, C- and P-conservation, the set of 14 couplings can be reduced to 5 parameters: $\mathrm{g_1^Z}$, κ_γ, κ_Z, λ_γ and λ_Z, with Standard Model values $\mathrm{g_1^Z} = \kappa_\mathrm{Z} = \kappa_\gamma = 1$ and $\lambda_\mathrm{Z} = \lambda_\gamma = 0$. Precision measurements at the Z resonance at LEP and SLC also provide bounds on the couplings [7, 8]. However, local $\mathrm{SU(2)_L \times U(1)_Y}$ gauge invariance reduces the relevance of these bounds [7] and introduces the constraints:

$$\Delta\kappa_\mathrm{Z} = -\Delta\kappa_\gamma \tan^2\theta_\mathrm{w} + \Delta\mathrm{g_1^Z},$$
$$\lambda_\mathrm{Z} = \lambda_\gamma,$$

where Δ denotes the deviation of the respective quantity from its non-zero Standard Model value, and θ_W is the weak mixing angle. Hence, only three parameters remain: $\mathrm{g_1^Z}$, κ_γ, and λ_γ [6].

In this note, the three couplings $\mathrm{g_1^Z}$, κ_γ and λ_γ are measured individually with the two other couplings fixed at zero, their Standard Model value. Fits are also presented, where two or all three couplings are allowed to vary.

This paper also presents new results from unconstrained single-parameter fits to the real and imaginary parts of the 6 C- and P-conserving TGCs, and updates previous results from single-parameter fits for the 8 TGCs which violate either C- or P-conservation.

Finally, limits are set on the mass and width of a techni-ρ resonance. If the Higgs boson is very heavy – or absent altogether – then $W_L^+W_L^-$ scattering becomes strong at high energies, where W_L denotes a longitudinally polarized W boson. In this paper the techni-ρ is defined to be the leading vector resonance in strong $W_L^+W_L^-$ scattering. In analogy with $e^+e^- \to \pi^+\pi^-$ and the ρ resonance, the effect of a techni-ρ resonance on $e^+e^- \to W_L^+W_L^-$ can be described by the complex technipion form factor F_T [9]

$$F_T = \frac{M_\rho^2 - i\Gamma_\rho M_\rho}{M_\rho^2 - s - i\Gamma_\rho M_\rho} \quad ,$$

where M_ρ and Γ_ρ are the mass and width of the techni-ρ, respectively. Limits are placed on M_ρ and Γ_ρ by measuring the real and imaginary parts of F_T.

A detailed description of the ALEPH detector is given in Ref. [10, 11].

2 Monte Carlo generators

Samples of fully simulated events, reconstructed with the same program as the data, are used for the design of the selections, determination of signal efficiencies and estimation of

the background contamination. The size of the generated signal samples corresponds to more than 300 times the collected luminosity.

The KORALW [12] program, which includes all four-fermion diagrams contributing to W^+W^--like final states, is used to generate the reference sample with a W mass of 80.35 GeV/c^2. The correction induced by improved calculations [13, 14] in the Double Pole Approximation [15] framework is computed for each event and applied by introducing an event weight. The KORALW generator is interfaced with JETSET [16], PHOTOS [17], and TAUOLA [18] for fragmentation, final state photon radiation and τ decays, respectively.

To include effects from various background processes, Monte Carlo samples are generated with a corresponding integrated luminosity of each background sample of at least 50 times that of the data. PYTHIA [16] is used to generate $e^+e^-\rightarrow$ZZ, Zee events. In the ZZ and Zee sample, events with W^+W^--like final states are discarded to avoid double counting. Two-photon processes are simulated with the PHOT02 [19] generator. Di-fermion final states are generated through KK2f [20] and BHWIDE [21] generators.

3 Event selection and kinematic reconstruction

The TGC measurement is a combination of cross-section and kinematical ones. A W-pair event can be characterized by five measured angles: θ_W, the W^- production angle between the W^- and the initial e^- in the W^+W^- rest frame, the polar and azimuthal angles of the lepton, $\theta^*_{\rm l}$ and $\phi^*_{\rm l}$, in the rest frame of its parent W and the polar and azimuthal angles of a quark jet, $\theta^*_{\rm jet}$ and $\phi^*_{\rm jet}$, in the rest frame of its parent W. Distributions of the five angles $\cos\theta_W$, $\cos\theta^*_l$, ϕ^*_l, $\cos\theta^*_{\rm jet}$ and $\phi^*_{\rm jet}$, for $e\nu q\bar{q}$ and $\mu\nu q\bar{q}$ events after selection and reconstruction are represented in Figure 1. Distributions of the reconstructed W^- production angle, θ_W, for $\tau\nu q\bar{q}$, $q\bar{q}q\bar{q}$ and $\ell\nu\ell\nu$ final states are shown in Figure 2.

The selection of candidate W^+W^- events with the topologies, $\ell\nu q\bar{q}$, $q\bar{q}q\bar{q}$, and $\ell\nu\ell\nu$, is similar to that used in the previous measurement of charged TGCs [1]. Selected events are exclusively classified in the following order of priority: $e\nu q\bar{q}$, $\mu\nu q\bar{q}$, $\tau\nu q\bar{q}$, $q\bar{q}q\bar{q}$, and $\ell\nu\ell\nu$. For the kinematical analysis, particles below 15 degrees (potentially affected by the superposition of beam-background) are removed from events.

4 Determination of the TGCs

An optimal observable analysis employing first and second order observables for W-pair production in the $\ell\nu q\bar{q}$, $q\bar{q}q\bar{q}$ and $\ell\nu\ell\nu$ final states, is used to measure the three TGCs g_1^Z, κ_γ and λ_γ. This method projects the sensitive kinematical information onto one dimensional distributions [22].

A maximum likelihood analysis is employed to provide the unconstrained one-parameter limits on the real and imaginary parts of the 14 TGCs and to perform the indirect search for the techni-ρ. For both analyses, additional information is also included from the measured total cross-section.

A detailed description of the optimal observable analysis of W-pair production final states and of the maximum likelihood analysis for $e\nu q\bar{q}$ and $\mu\nu q\bar{q}$ final states can be found in Ref. [2]. A description of the maximum likelihood analysis for $\tau\nu q\bar{q}$, $q\bar{q}q\bar{q}$ and $\ell\nu\ell\nu$ final states can be found in Ref. [1] .

Table 1: Summary of systematic uncertainties for all WW channels combined estimated at 189 GeV for the couplings g_1^Z, κ_γ and λ_γ. A detailed description of the different sources is given in Ref. [2]. Systematic uncertainties below 0.001 are indicated by a dash.

Source	g_1^Z	κ_γ	λ_γ
Luminosity	0.002	0.026	0.009
LEP energy	0.001	0.002	0.001
WW cross section	0.002	0.017	0.006
WW shape	0.010	0.020	0.010
W mass	-	-	-
Fragmentation	0.005	0.013	0.001
Background	0.002	0.020	0.002
Tracking	0.002	0.004	0.001
Calorimeter	0.003	0.004	0.002
Bose-Einstein	0.010	0.018	0.002
Colour-Reconnection	0.008	0.016	0.005
MC statistics	0.003	0.013	0.002

4.1 Systematic uncertainties

All systematic uncertainties are evaluated with Monte-Carlo samples simulated at 189 GeV and used at all energies. Only Monte Carlo statistical error is estimated separately for each centre-of-mass energy. In this note, the uncertainty on the $O(\alpha)$ correction to the 'WW shape' is evaluated following the method presented in Ref. [23]. The quoted numbers are the one agreed inside the LEP-TGC Working Group. The other systematics were described in [1]. The different contributions of each source to the total systematic error for the three couplings g_1^Z, κ_γ and λ_γ, as obtained with the OO method, are given for all WW channels combined in Table 1. The systematic uncertainties for the technipion form factor F_T and the unconstrained fits of the 6 C- and P-conserving TGCs are shown in Table 2, while the systematic errors for the 8 TGCs that violate either C- or P-conservation are displayed in Table 3.

5 Results

5.1 Results for WW channel with LEP2 data

The combined results from all W^+W^- decay channels from 183 to 209 GeV for the three couplings g_1^Z, κ_γ and λ_γ, are obtained with the OO analysis. The correlation of the systematic errors between the different channels and energies are included as described in Ref. [2]. The results for g_1^Z, κ_γ and λ_γ, including systematic uncertainties, are:

$$\begin{aligned} g_1^Z &= 1.030^{+0.035}_{-0.034} \\ \kappa_\gamma &= 1.029^{+0.097}_{-0.082} \\ \lambda_\gamma &= 0.014^{+0.034}_{-0.033}, \end{aligned}$$

The corresponding $\log L$ curves splitted between $q\bar{q}q\bar{q}$, $\ell\nu q\bar{q}$ and $\ell\nu\ell\nu$ are shown in Figure 3.

In all cases described above, each coupling is determined fixing the other couplings to their Standard Model values. The error intervals for each coupling are defined as the 68% confidence level intervals obtained by integration of the likelihood functions, to accommodate cases with non-parabolic behaviour of the log-likelihood function.

5.2 Combined TGC results for 183-209 GeV

Measurements from W-pair production at all LEP2 energies are combined with results from single-W production at 183-202 GeV [3], and single-γ production at 183-209 GeV [1]. The combined results for g_1^Z, κ_γ and λ_γ are listed in Table 4 and corresponding one-parameter $\log L$ curves are shown in Figure 4.

To study the full correlation between parameters, two- and three-parameter fits, where two or all three couplings are allowed to vary, are also presented. Fits use the combined information from W-pair production at 183-209 GeV single-W production at 183-202 GeVand single-γ production at 183-209 GeV.

For the three parameter fit, results and errors computed for ΔL_{min}=0.5 are summarised in Table 5 including the systematic uncertainties. Three-parameter fit correlation matrix is also given in Table 5. This correlation matrix is evaluated at the local minimum.

Projections onto two dimensional planes of the three dimensional envelope of the 95% confidence level volume, representing the integration of the confidence over the corresponding third coupling, are shown in Figure 5. 95% confidence limits of the respective 2-parameter fits of the three pairs of couplings (g_1^Z, κ_γ), (g_1^Z, λ_γ) and (κ_γ, λ_γ) are shown as dashed lines. Systematic uncertainties are included in the given limits.

5.3 Unconstrained one-parameter fits of all 14 TGCs

Results from the unconstrained one-parameter fits of the real and imaginary parts of the six TGCs that are both C- and P-conserving are given in Table 6. Here unconstrained means that no relationship between the TGCs is assumed. The only assumption is that all TGCs are fixed at their Standard Model values, with the exception of the fitted TGC.

The results from the one-parameter fits of the real and imaginary parts of the 8 TGCs that violate either C- or P-conservation are shown in Table 7. Of these 8 TGCs, 6 are CP-violating while two – g_5^γ and g_5^Z — conserve CP.

Table 2: Summary of the systematic uncertainties for the technipion form factor F_T and for the unconstrained one-parameter fits of the 6 C- and P-conserving TGCs. A detailed description of the different sources is given in Ref. [2]. Systematic uncertainties below 0.001 are indicated by a dash.

	Real							Imaginary						
Source	κ_γ	λ_γ	g_1^γ	κ_Z	λ_Z	g_1^Z	F_T	κ_γ	λ_γ	g_1^γ	κ_Z	λ_Z	g_1^Z	F_T
LEP energy	.007	.006	.008	.001	.004	.003	.001	.004	.002	.003	.002	.001	.001	.001
Luminosity	.008	.005	.012	.002	.001	.001	.012	.004	-	.002	.003	-	.001	.006
WW cross section	.007	.003	.009	.001	.001	.001	.011	.004	-	.001	.002	-	.001	.006
WW shape	.005	.004	.001	.004	.001	.004	-	-	.007	.002	-	.001	.003	.004
Fragmentation	.023	.002	.015	.014	.002	.009	.002	.009	.001	.006	.005	.002	.005	.001
Background	.016	.028	.046	.020	.009	.008	.027	.029	.023	.016	.018	.011	.012	.027
Tracking	.008	.001	.005	-	-	-	.005	.005	-	.002	.003	.001	.002	.008
Calorimeter	.004	.001	.002	.010	.011	.011	.004	.002	.015	.014	.001	.010	.008	.012
MC Statistics	.002	-	.001	.003	.002	.001	.009	.009	.008	.012	.007	.004	.007	.016
Bose-Einstein	.001	.004	.002	.015	.001	.012	-	.009	.005	.009	.005	.004	.005	-
Color-Reconnection	.004	.010	.005	.012	.007	.004	-	.001	.008	.003	-	.006	.003	.006
Total	.033	.031	.051	.033	.017	.022	.033	.034	.031	.027	.021	.017	.018	.036

Table 3: Summary of the systematic uncertainties for the one-parameter fits of the 8 TGCs that violate C or P conservation. A detailed description of the different sources is given in Ref. [2]. Systematic uncertainties below 0.001 are indicated by a dash.

	Real								Imaginary							
Source	$\tilde{\kappa}_\gamma$	$\tilde{\lambda}_\gamma$	$\tilde{\kappa}_Z$	$\tilde{\lambda}_Z$	g_4^γ	g_5^γ	g_4^Z	g_5^Z	$\tilde{\kappa}_\gamma$	$\tilde{\lambda}_\gamma$	$\tilde{\kappa}_Z$	$\tilde{\lambda}_Z$	g_4^γ	g_5^γ	g_4^Z	g_5^Z
LEP energy	.003	.003	.001	.002	.007	.005	.004	.005	.001	.001	-	-	.002	.011	.003	.005
Luminosity	.008	.006	.005	.004	.004	.009	.007	.002	.001	.001	.001	.001	.002	.011	.003	.004
WW cross section	.006	.005	.004	.003	.003	.007	.005	.002	.001	.001	.001	.001	.002	.009	.003	.003
WW shape	.001	.001	.001	.002	.007	.004	.002	.004	.001	-	.001	.001	.008	.001	.003	.003
Fragmentation	.003	.008	.003	-	.014	.056	.010	.039	.010	.007	.010	.007	.007	.051	.014	.040
Background	.031	.029	.016	.015	.038	.015	.028	.011	.006	.005	.002	.001	.022	.056	.009	.012
Tracking	-	-	.001	-	.004	.018	.004	.015	.001	.001	.001	.001	.007	.005	.002	.002
Calorimeter	.024	.011	.006	.002	.018	.062	.002	.026	.002	.003	.001	.001	-	.020	.031	.017
MC Statistics	.008	.004	-	-	.002	.023	.010	.006	.009	.008	.001	.002	.033	.003	.015	.009
Bose-Einstein	.006	.005	.001	.001	.019	.007	.011	.002	.009	.006	.006	.004	.009	.006	.004	.003
Color-Reconnection	.007	.006	.004	.003	.002	.003	.002	.001	.015	.016	.020	.018	.009	.001	-	.005
Total	.043	.034	.020	.017	.050	.091	.035	.051	.023	.021	.023	.020	.044	.080	.038	.047

Table 4: Combined results for g_1^Z, κ_γ and λ_γ from W^+W^- production at 183-209 GeV, single-γ at 183-209 GeV and single-W production at 183-202 GeV. Each coupling is determined fixing the two other couplings to their Standard Model value (1D fit). The errors include systematic uncertainties. The corresponding 95% confidence level intervals are listed in the last column.

Coupling	Fit result	95% confidence limits
g_1^Z	$1.030^{+0.035}_{-0.034}$	[0.965 , 1.099]
κ_γ	$0.990^{+0.072}_{-0.068}$	[0.861 , 1.140]
λ_γ	$0.014^{+0.033}_{-0.032}$	[-0.048 , 0.081]

Table 5: Result of a three-parameter fit for g_1^Z, κ_γ and λ_γ using the combined information from W-pair production at 183-209 GeV, single-γ at 183-209 GeV and single-W production at 183-202 GeV. The statistical and systematic uncertainties are combined in a ΔL_{min}=0.5 error. The corresponding correlations are given in the last column.

		Correlation		
Coupling	fit result	g_1^Z	κ_γ	λ_γ
g_1^Z	$1.045^{+0.040}_{-0.042}$	1.0	-0.15	-0.63
κ_γ	$0.984^{+0.066}_{-0.062}$		1.0	-0.15
λ_γ	$-0.008^{+0.042}_{-0.042}$			1.0

5.4 The technipion form factor F_T and the techni-ρ mass

The results for the one-parameter fits of the real and imaginary parts of the technipion form factor F_T are shown in Table 6. The imaginary part of F_T is fixed at 0 when fitting $Re(F_T)$ while the real part of F_T is fixed at 1 while fitting $Im(F_T)$.

In order to convert the measurement of F_T into limits on the techni-ρ mass and width it will be assumed that $M_\rho >> \sqrt{s}$. This assumption leads to the following expression for F_T:

$$F_T = 1 + (1+r^2)^{-1}\frac{s}{M_\rho^2}(1+ir)$$

where $r = \Gamma_\rho/M_\rho$. Hence the true values of $\Delta Re(F_T) = Re(F_T) - 1$ and $Im(F_T)$ are always positive when $M_\rho >> \sqrt{s}$. Another consequence of the assumption $M_\rho >> \sqrt{s}$ is that the one-parameter fit of $Re(F_T)$ is independent of the true value of $Im(F_T)$ and vice versa. This in turn implies that the means and variances of the one-parameter fits for $Re(F_T)$ and $Im(F_T)$ can be used to form a binormal distribution of $Re(F_T)$ and $Im(F_T)$. The 95% C.L. contour for this binormal distribution is shown in Fig. 6a. The solid black region in Fig. 6a indicates the allowed region assuming $M_\rho >> \sqrt{s}$. Points uniformly distributed within the solid black region of Fig. 6a have been mapped onto the $(M_\rho, \Gamma\rho/M_\rho)$ plane in Fig. 6b. The shaded region in Fig. 6b is thus allowed at 95% C.L., while the solid white region in Fig. 6b is excluded at 95% C.L. The results from Fig. 6b imply $M_\rho > 725\ GeV$ at 95% C.L. assuming

coupling	fit result	95% confidence limits
$\Delta Re(\kappa_\gamma)$	$0.071^{+0.063}_{-0.061}$	[-0.047, 0.196]
$Re(\lambda_\gamma)$	$0.096^{+0.072}_{-0.069}$	[-0.037, 0.238]
$\Delta Re(g_1^\gamma)$	$0.123^{+0.093}_{-0.090}$	[-0.052, 0.308]
$\Delta Re(\kappa_Z)$	$0.065^{+0.062}_{-0.061}$	[-0.055, 0.186]
$Re(\lambda_Z)$	$0.019^{+0.054}_{-0.054}$	[-0.086, 0.124]
$\Delta Re(g_1^Z)$	$0.066^{+0.073}_{-0.072}$	[-0.075, 0.210]
$\Delta Re(F_T)$	$-0.034^{+0.055}_{-0.056}$	[-0.144, 0.073]
$\Delta Im(\kappa_\gamma)$	$0.070^{+0.090}_{-0.092}$	[-0.111, 0.245]
$Im(\lambda_\gamma)$	$0.002^{+0.072}_{-0.072}$	[-0.138, 0.142]
$\Delta Im(g_1^\gamma)$	$0.030^{+0.103}_{-0.103}$	[-0.173, 0.230]
$\Delta Im(\kappa_Z)$	$0.053^{+0.060}_{-0.061}$	[-0.067, 0.169]
$Im(\lambda_Z)$	$0.003^{+0.046}_{-0.046}$	[-0.087, 0.093]
$\Delta Im(g_1^Z)$	$0.023^{+0.069}_{-0.069}$	[-0.111, 0.157]
$\Delta Im(F_T)$	$-0.147^{+0.098}_{-0.097}$	[-0.335, 0.046]

Table 6: *Results from WW events at 183-209 GeV for the real and imaginary parts of the TGCs that are both C- and P- conserving. Also shown are the results for the real and imaginary parts of the technipion form factor F_T. Each coupling has been determined using a one-parameter maximum likelihood fit with all other couplings fixed at their Standard Model value. The error quoted is the 68% error obtained by integration of the likelihood functions including systematic uncertainties. The corresponding 95% confidence intervals are listed in the last column.*

$\Gamma_\rho/M_\rho < 0.5$. The techni-ρ mass limit is reduced to $M\rho > 625$ GeV at 95% C.L if values for the width as large as $\Gamma_\rho/M_\rho = 1.0$ are allowed.

6 Summary and conclusion

Triple gauge-boson couplings have been measured using W-pair events collected by ALEPH at centre-of-mass energies between 183 and 209 GeV corresponding to an integrated luminosity of 684 pb^{-1}. Combined with previous results from single-W production and

coupling	fit result	95% confidence limits
$Re(\tilde{\lambda}_\gamma)$	$0.059^{+0.090}_{-0.092}$	[-0.120, 0.231]
$Re(\tilde{\kappa}_Z)$	$-0.089^{+0.066}_{-0.064}$	[-0.214, 0.041]
$Re(\tilde{\lambda}_Z)$	$0.064^{+0.049}_{-0.051}$	[-0.036, 0.159]
$Re(g_4^\gamma)$	$0.058^{+0.165}_{-0.167}$	[-0.269, 0.377]
$Re(g_5^\gamma)$	$-0.043^{+0.208}_{-0.210}$	[-0.455, 0.362]
$Re(g_4^Z)$	$0.134^{+0.110}_{-0.112}$	[-0.087, 0.347]
$Re(g_5^Z)$	$-0.064^{+0.128}_{-0.128}$	[-0.315, 0.188]
$Im(\tilde{\kappa}_\gamma)$	$-0.036^{+0.061}_{-0.061}$	[-0.156, 0.084]
$Im(\tilde{\lambda}_\gamma)$	$0.041^{+0.048}_{-0.048}$	[-0.054, 0.135]
$Im(\tilde{\kappa}_Z)$	$-0.034^{+0.044}_{-0.044}$	[-0.120, 0.052]
$Im(\tilde{\lambda}_Z)$	$0.032^{+0.035}_{-0.035}$	[-0.037, 0.100]
$Im(g_4^\gamma)$	$0.051^{+0.144}_{-0.144}$	[-0.229, 0.332]
$Im(g_5^\gamma)$	$-0.169^{+0.247}_{-0.245}$	[-0.644, 0.316]
$Im(g_4^Z)$	$0.102^{+0.096}_{-0.097}$	[-0.089, 0.290]
$Im(g_5^Z)$	$-0.074^{+0.154}_{-0.153}$	[-0.372, 0.227]

Table 7: *Results from WW events at 183-209 GeV for the real and imaginary parts of TGCs that violate either C- or P-conservation. Each coupling has been determined using a one-parameter maximum likelihood fit with all other couplings fixed at their Standard Model value. The error quoted is the 68% error obtained by integration of the likelihood functions including systematic uncertainties. The corresponding 95% confidence intervals are listed in the last column.*

single-γ production, the three couplings g_1^Z, κ_γ and λ_γ have been measured individually, assuming the two other couplings to be fixed at their Standard Model value. Results are

$$\begin{aligned} g_1^Z &= 1.030^{+0.035}_{-0.034} \\ \kappa_\gamma &= 0.990^{+0.072}_{-0.068} \\ \lambda_\gamma &= 0.014^{+0.033}_{-0.032}, \end{aligned}$$

where errors include systematic uncertainties. Corresponding 95% confidence level limits,

$$0.965 < \quad g_1^Z \quad < \quad 1.099$$

$$0.861 < \quad \kappa_\gamma \quad < \quad 1.140$$

$$-0.048 < \quad \lambda_\gamma \quad < \quad 0.081,$$

are in good agreement with Standard Model expectation. Multi-parameter fits, where two or all three couplings are allowed to vary show also good agreement with the Standard Model expectations.

In addition, ALEPH measured separately the real and imaginary parts of all 14 TGCs parameters. No deviation from the Standard Model expectation is observed and limits are summarized in Table 6 and Table 7.

Finally, WW pair production provided a tool to test the existence of a techni-ρ resonance through $W_L^+W_L^-$ production. No deviation from the Standard Model is observed and the 95% confidence level limits on the associated techni-pion form factor are:

$$-0.144 < \quad \Delta Re(F_T) \quad < \quad 0.073$$

$$-0.335 < \quad \Delta Im(F_T) \quad < \quad 0.046$$

This is translated in a lower limit on the techni-ρ mass of 625 GeV.

7 Acknowledgements

We would like to thank the YFSWW group for useful discussions on the estimation of the effect of the improved $\mathcal{O}(\alpha)$ calculation with the KORALW Monte Carlo. It is a pleasure to congratulate our colleagues from the CERN accelerator divisions for the highly successful operation of LEP at high energies. We are indebted to the engineers and technicians in all our institutions for the contributions to the excellent performance of ALEPH. Those of us from non-member countries thank CERN for its hospitality.

References

[1] ALEPH Collaboration, *Measurement of Triple Gauge-Boson Couplings in* e^+e^- *collisions up to 208 GeV*, contributed paper to the 2001 Summer Conferences, ALEPH 2001-060, CONF 2001-040.

[2] ALEPH Collaboration,*Measurement of Triple Gauge-Boson Couplings at LEP energies up to 189 GeV* Eur. Phys. J. C21 (2001) 423.

[3] ALEPH Collaboration, *Single W Production at Energies up to* $\sqrt{s}$ *= 202 GeV and Search for Anomalous Triple Gauge Boson Couplings*, contributed paper to the ICHEP2000, ALEPH 2000-054, CONF 2000-036.

[4] K. Hagiwara, R. D. Peccei, D. Zeppenfeld and K. Hikasa, Nucl. Phys. B282 (1987) 253.

[5] M. Bilenky, J.L. Kneur, F.M. Renard and D. Schildknecht, Nucl. Phys. B409 (1993) 22.

[6] G. Gounaris, J.-L. Kneur and D. Zeppenfeld, from *Physics at LEP2*, CERN 96-01 p. 525, editors G. Altarelli, T. Sjöstrand and F. Zwirner.

[7] A. De Rújula, M. B. Gavela, P. Hernandez and E. Massó, Nucl. Phys. B384 (1992) 3.

[8] J. Ellison and J. Wudka, Ann. Rev. Nucl. Part. Sci. 48 (1998) 33.

[9] T. L. Barklow *et al.*, arXiv:hep-ph/9704217.

[10] ALEPH Collaboration, *ALEPH: A Detector for Electron-Positron Annihilations at LEP*, Nucl. Instrum. and Methods A 294 (1990) 121.

[11] ALEPH Collaboration, *Performance of the ALEPH Detector at LEP*, Nucl. Instrum. and Methods A 360 (1995) 481.

[12] M. Skrzypek, S. Jadach, W. Placzek and Z. Wąs, Comp. Phys. Commun. 94 (1996) 216.

[13] S. Jadach, W. Placzek, M. Skrzypek, B. F. L. Ward and Z. Wąs, Phys. Lett. B417 (1998) 326;CERN-TH/1999-222, UTHEP-98-0502.

[14] A. Denner, S. Dittmaier, M. Roth and D. Wackeroth, BI-TP 99/45, hep-ph/9912261 (1999).

[15] W. Beenakker, F. A. Berends and A. P. Chapowsky, Nucl. Phys. B548 (1999) 3.

[16] T. Sjöstrand, Comp. Phys. Commun. 82 (1994) 74.

[17] E. Barberio *et al.*, Comp. Phys. Commun. 67 (1991) 115, Comp. Phys. Commun. 79 (1994) 291.

[18] S. Jadach *et al.*, Comp. Phys. Commun. 70 (1992) 69, Comp. Phys. Commun. 76 (1993) 361.

[19] ALEPH Collaboration, *An Experimental Study of $\gamma\gamma \rightarrow$Hadrons at LEP*, Phys. Lett. B313 (1993) 509;
J. A. M. Vermasseren in *Proceedings of the IVth International Workshop on Gamma-Gamma Interactions*, Eds. G. Cochard and P. Kessler, Springer Verlag (1980).

[20] The precision Monte Carlo event generator KK for two-fermion final states in e+ e-collisions, S. Jadach, B.F.L. Ward and Z. Wąs, Comput. Phys. Commun. **130** (2000) 260-325.

[21] S. Jadach, W. Placzek and B. F. L. Ward, Phys. Lett. B390 (1997) 298.

[22] M. Diehl and O. Nachtmann, Zeit. Phys. C62 (1994) 397;
D.K. Fanourakis, D. Fassouliotis and S.E. Tzamarias, Nucl. Instrum. and Methods A412 (1998) 465; Nucl. Instrum. and Methods A414 (1998) 399.

[23] R. Brunelière et al *On theoretical uncertainties of the W angular distribution in W pair production at LEP2*, Phys. Lett. B533 (2002) 75.

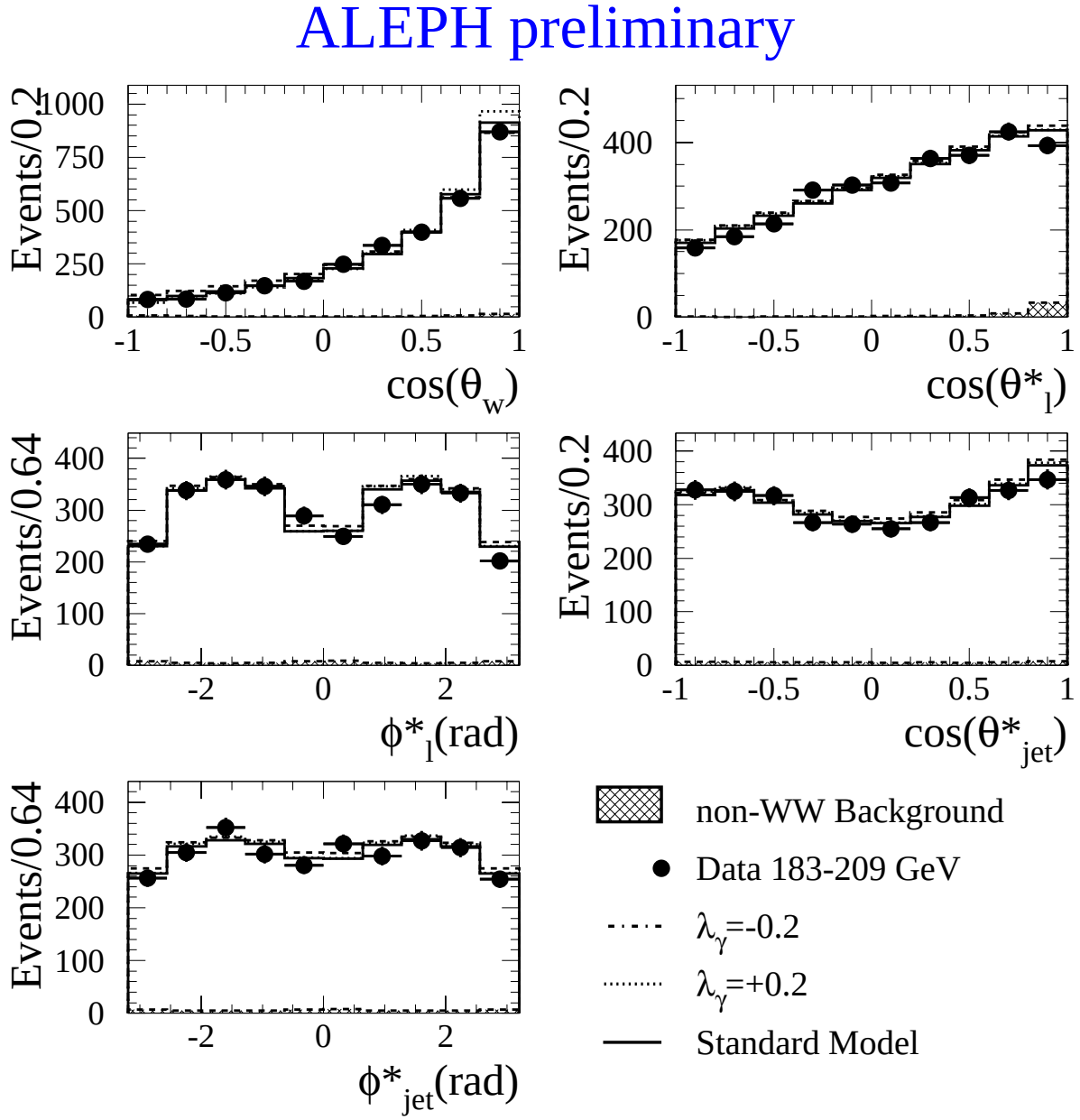

Figure 1: Combined $e\nu q\bar{q}$ and $\mu\nu q\bar{q}$ channels distributions of the kinematical quantities $\cos\theta_W$, $\cos\theta_l^*$, ϕ_l^*, $\cos\theta_{\rm jet}^*$ and $\phi_{\rm jet}^*$ for all energies above 183 GeV. The measured variables are the angle θ_W between the $\rm W^-$ and initial e^- in the $\rm W^+W^-$ rest frame, the polar and azimuthal angles of the lepton, $\theta_{\rm l}^*$ and $\phi_{\rm l}^*$, in the rest frame of its parent W, and the polar and azimuthal angles of a quark jet, $\theta_{\rm jet}^*$ and $\phi^*{}_{\rm jet}$, in the rest frame of its parent W. As no quark flavour tagging is performed each of the two ambiguous solutions enters with a weight of 0.5. Data are represented by solid dots, while the solid and dashed histograms show distributions for Standard Model and non-standard values of $\lambda_\gamma = \pm 0.2$.

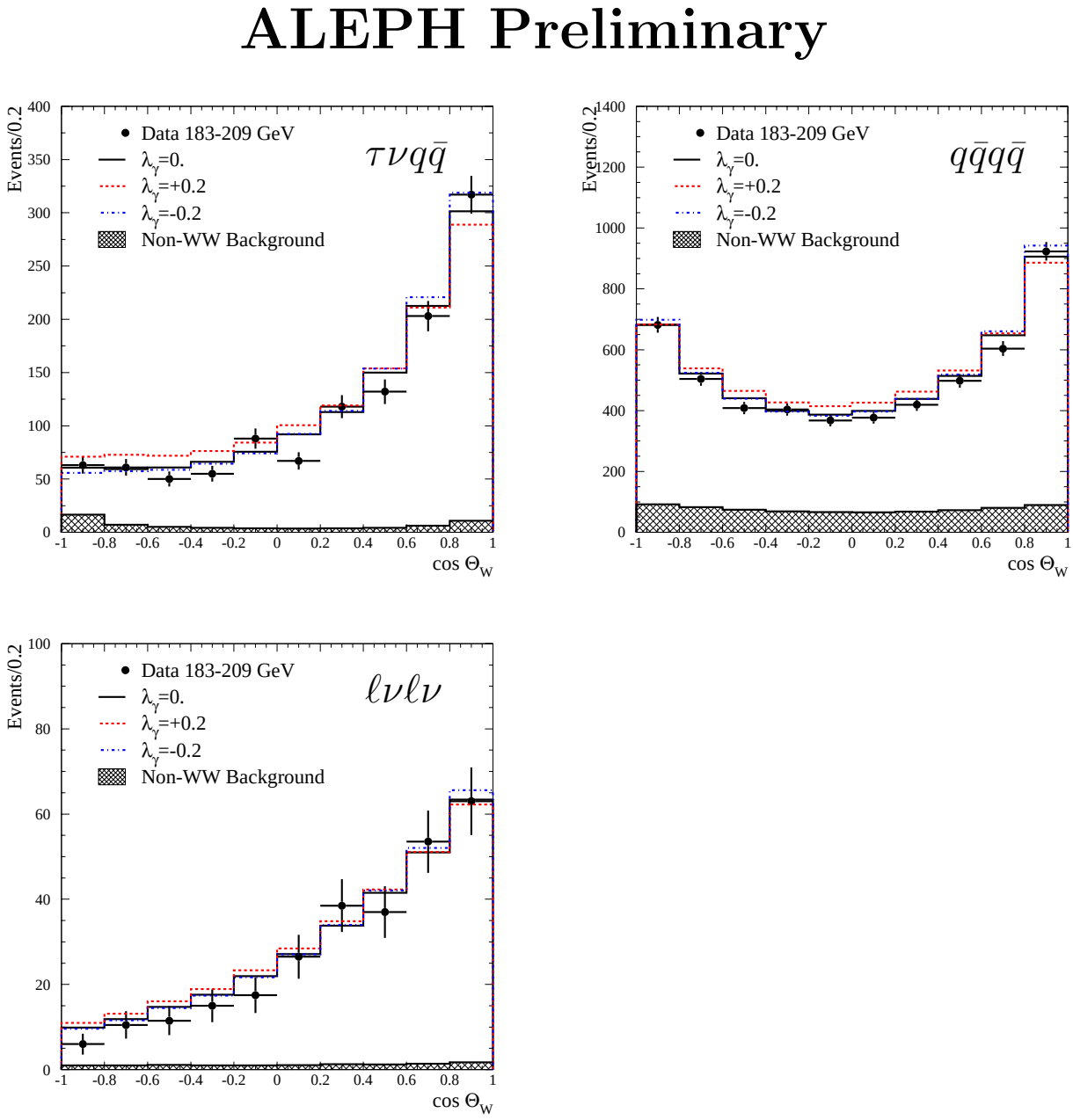

Figure 2: Distributions of the cosine of the W^- production angle, $\cos\theta_W$, at LEP2 for $\tau\nu q\bar{q}$, $q\bar{q}q\bar{q}$ and $\ell\nu\ell\nu$ events. Data are represented by solid dots, while the solid and dashed/dotted-dashed histograms show distributions for Standard Model and non-standard values of the TGCs. The shaded area represents the non-WW background. For $q\bar{q}q\bar{q}$ events, each event enters with two solutions for $\cos\theta_W$ in the distribution with the weights P_+ and $1 - P_+$, where P_+ is the probability for a di-jet pair to be a W^+ [2]. For $\ell\nu\ell\nu$ events, each event enters with two solutions for $\cos\theta_W$ in the distribution with a weight of 0.5.

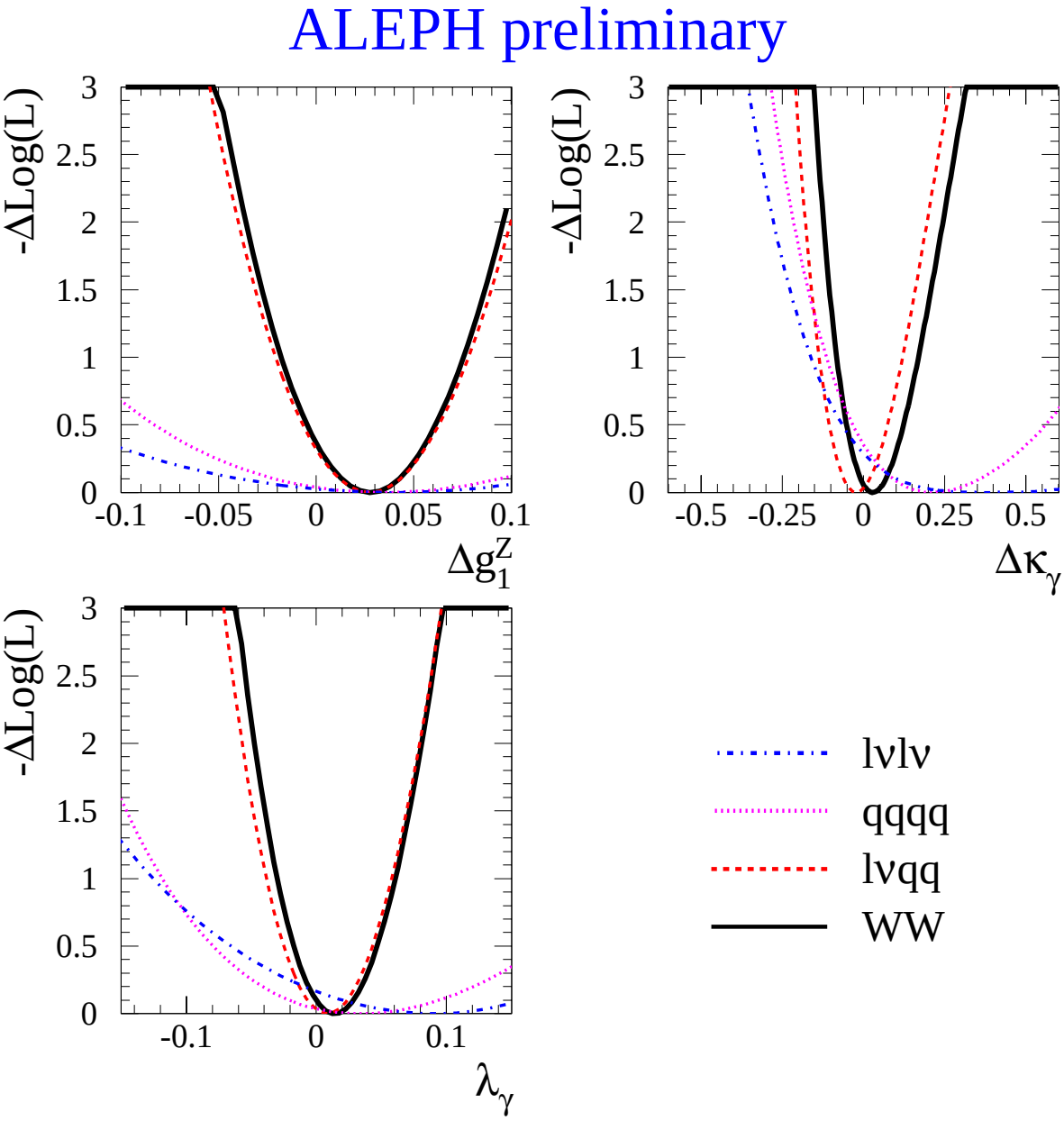

Figure 3: The combined negative log-likelihood curves from the W-pair analysis including all LEP2 data for the individual fits in the $\ell\nu q\bar{q}$ (dashed), $q\bar{q}q\bar{q}$ (light grey) and $\ell\nu\ell\nu$ (dashed-dotted) channels for the three couplings Δg_1^Z, $\Delta\kappa_\gamma$ and λ_γ. The combined result is shown as the solid curve. The curve for each coupling is obtained while fixing the other couplings to their Standard Model value. The systematic uncertainties are included.

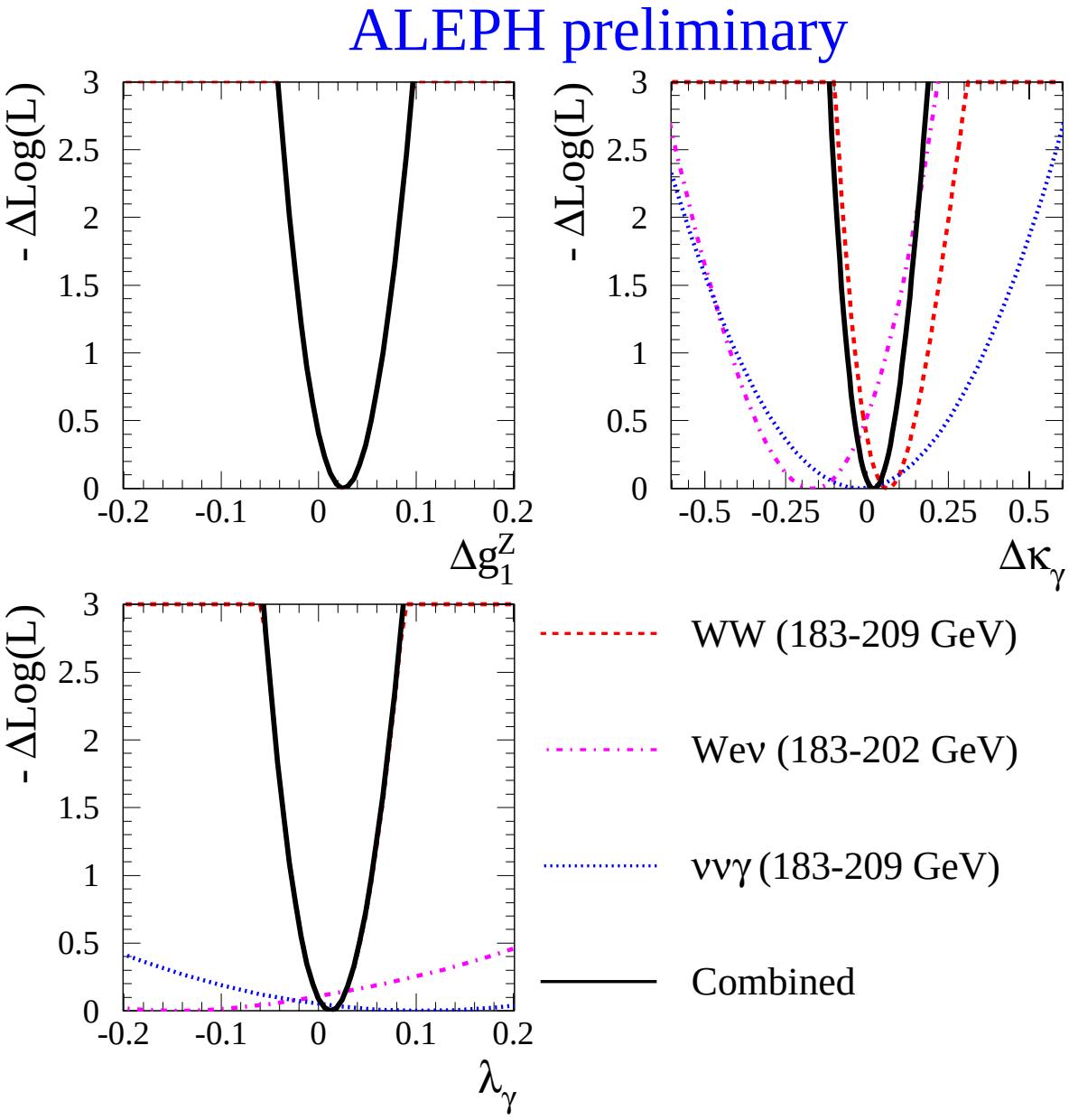

Figure 4: The negative log-likelihood curves for the combined fits using information from single-γ (dotted) production at 183-209 GeV, single-W (dashed-dotted) production at 183-202 GeV and W-pair (dashed) production at energies up to 209 GeV for the three couplings Δg_1^Z, $\Delta\kappa_\gamma$ and λ_γ. The curve for each coupling is obtained while fixing the other couplings to their Standard Model value. The systematic uncertainties are included. The combined result is shown as the solid curve.

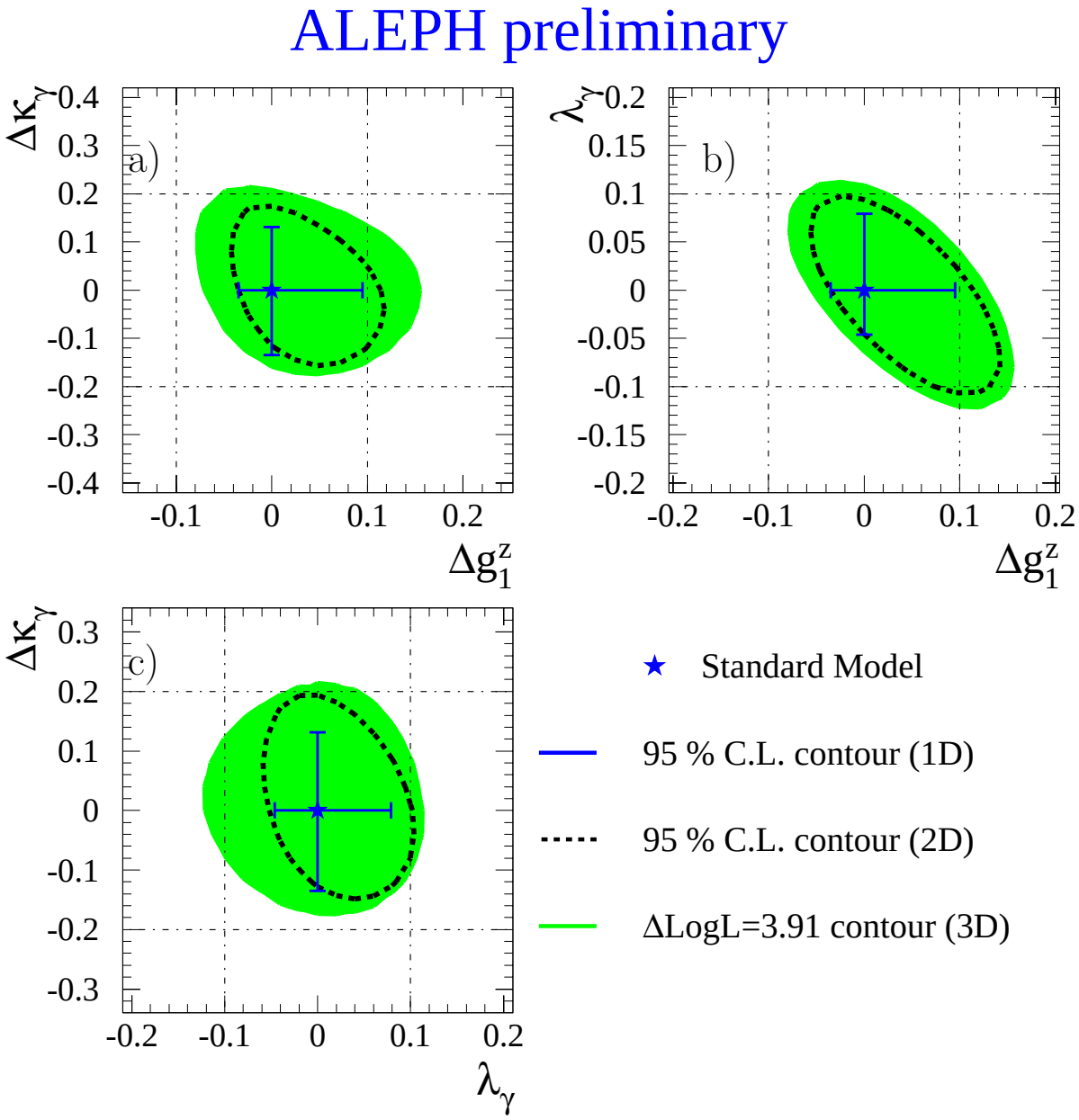

Figure 5: Multi-parameter fits using the combined data from single-γ production at 183-209 GeV, single-W production at 183-202 GeV and W-pair production at energies up to 209 GeV. The two-dimensional 95% confidence level contours for the three pairs of couplings, a) (Δg_1^Z, $\Delta\kappa_\gamma$), b) (Δg_1^Z, λ_γ) and c) ($\Delta\kappa_\gamma$, λ_γ). The solid straight line indicates the limits of the 95 % limits for the single parameter fit assuming the two others at their Standard Model value. The dashed lines show the 95% confidence level contours of the two-parameter fit. The shaded area is a projection onto the two-dimensional plane of the three-dimensional envelope of the 95% confidence level volume. The Standard Model point is represented by a star.

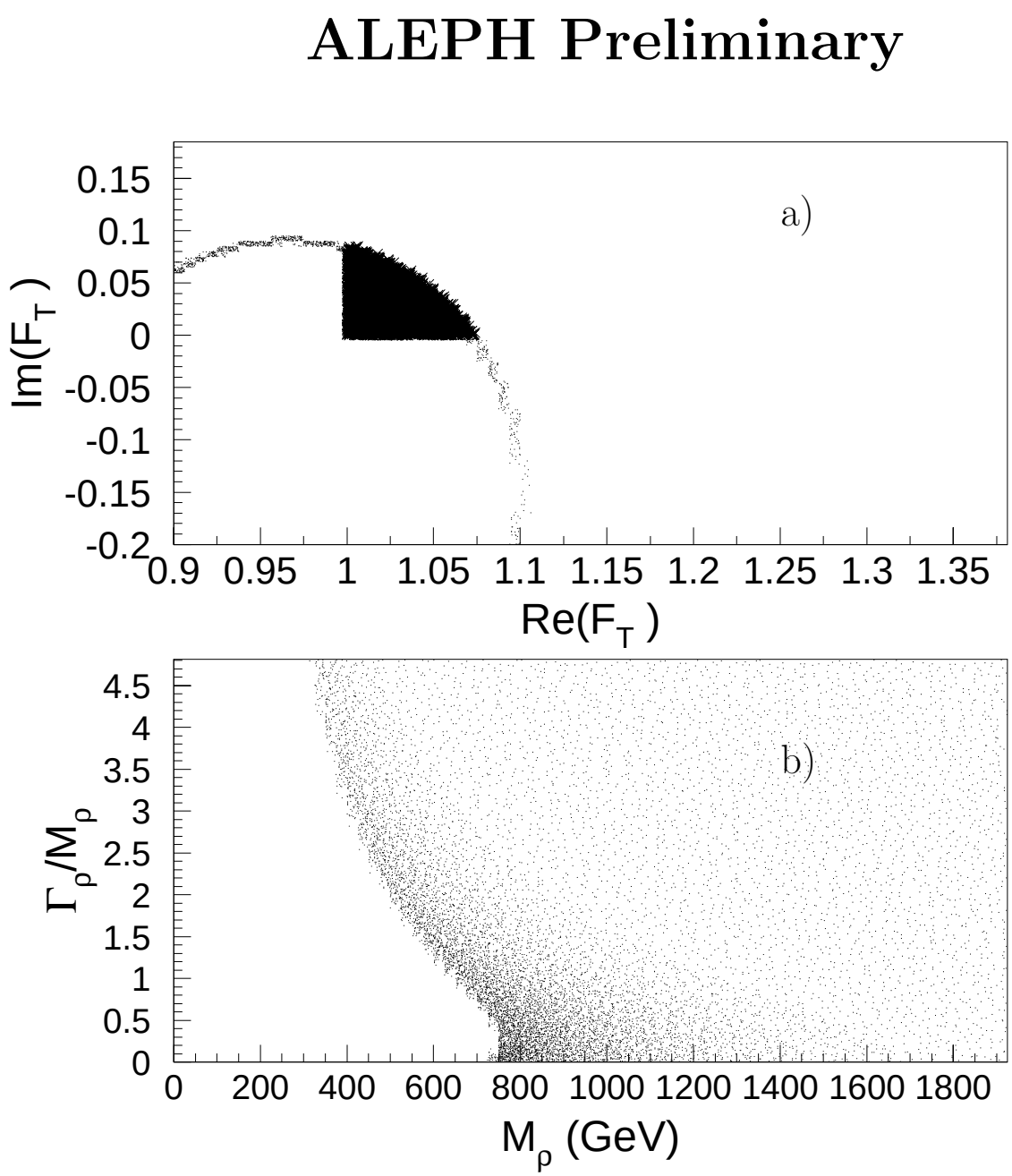

Figure 6: In (a) the 95% C.L. ellipse for the real and imaginary parts of the technipion form factor F_T is shown centered on $(Re(F_T), Im(F_T)) = (0.97, -0.15)$. The solid black area within the ellipse indicates the allowed region with $Re(F_T), Im(F_T) > 0$. Points distributed uniformly within the solid black area of (a) are mapped onto the $(M_\rho, \Gamma_\rho/M_\rho)$ plane in (b) according to the expression for F_T in Section 5.4. The white region in (b) is thus excluded at 95% C.L..